Chapter 12
Propagation Effects Caused by Finitely Conducting Ground on Lightning Return Stroke Electromagnetic Fields

12.1 Introduction

Consider a radio antenna located over ground and transmitting at a given frequency. If the ground is perfectly conducting, the amplitude of the radio wave generated by the antenna decreases inversely with distance as one moves away from the antenna, i.e., the signal decreases as $1/r$, where r is the distance from the antenna to the point of observation. However, if the conductivity of the ground is finite, then the amplitude of the radio wave decreases much more rapidly than the inverse distance. The higher the frequency of the wave, the higher the rate of decrease of the radio signal with distance. This attenuation of the radio signal or the electromagnetic wave by finitely conducting ground is called *propagation effects*. Attenuation of the electromagnetic wave results from the absorption of energy from the electromagnetic field by the finitely conducting ground. The higher the frequency of the electromagnetic field, the higher the amount of energy absorbed by the ground. Let us analyze this a bit further. Consider an electromagnetic field generated by a radio antenna tuned to a given frequency. If the ground is perfectly conducting, at any given point on the ground the electric field is perpendicular to the ground surface and the magnetic field is in the azimuthal direction (Fig. 12.1a). The direction of energy flow or the Poynting vector (i.e., $\mathbf{E} \times \mathbf{H}$) of the electromagnetic field at that point is directed parallel to the ground. Now consider the electromagnetic field of a radio antenna located over finitely conducting ground. In this case, the magnetic field has the same direction as before, but the electric field is inclined to the surface of the ground (Fig. 12.1b). That is, there is a component of the electric field parallel to the ground. This component is called the *horizontal electric field*. The Poynting vector in this case is directed towards the ground (a component of which is directed into the ground), indicating that energy is absorbed from the electromagnetic field by the ground. With increasing frequency or with decreasing ground conductivity the angle between the vertical and the direction of the

V. Cooray, *An Introduction to Lightning*,
DOI 10.1007/978-94-017-8938-7_12

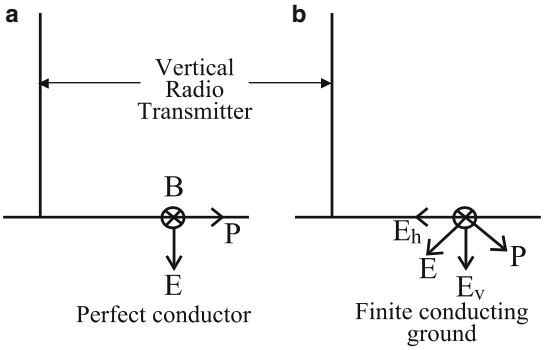

Fig. 12.1 (**a**) The electric field vector **E** over perfectly conducting ground is perpendicular to the ground surface, and the Poynting vector **P** [which is equal to $\frac{1}{\mu_0}(\mathbf{E} \times \mathbf{B})$] is parallel to the surface. The magnetic field **B** is azimuthal and goes into the plane. (**b**) Over finitely conducting ground the electric field vector is inclined to the ground surface (the magnetic field has the same direction), and the Poynting vector is directed towards the ground (a component of which is directed into the ground). Thus, in the case of finitely conducting ground, energy is absorbed by the ground from the electromagnetic field (Figure created by author)

electric field increases, i.e., the horizontal electric field increases. Thus, the energy absorbed by the ground increases with increasing frequency and with decreasing conductivity.

In the case of lightning-generated electromagnetic fields, which contain all the frequencies by differing amounts, the higher frequencies are selectively attenuated by ground, and as a result the fast or rapid features of the electromagnetic field disappear as the distance of propagation increases. The effect of this selective attenuation of higher frequencies is to increase the rise time and decrease the amplitude of the electromagnetic field (Sect. 12.3). Interestingly, in the case of lightning generated electric fields the Poynting vector rotates with time having a direction towards the ground at short times and becoming more and more parallel to ground with increasing time.

Knowledge concerning the characteristics of electromagnetic fields generated by lightning flashes is of importance in evaluating the interaction of these electromagnetic fields with electrical networks and in the remote sensing of lightning current parameters from the measured fields. However, as described previously, electromagnetic fields generated by lightning change their character as they propagate over the ground surface because of selective attenuation of high-frequency signals by finitely conducting ground. Thus, the peak and rise time of lightning-generated electric fields and electric field time derivatives measured at a given distance from the lightning channel may deviate more or less from the values that would be present over perfectly conducting ground depending on the distance of propagation and the conductivity of the ground.

In this chapter a simple procedure to evaluate propagation effects on electromagnetic fields generated by lightning return strokes is described.

12.2 Theory

In Chap. 3 we derived an expression for an electromagnetic field generated by a Hertzian dipole located above a perfectly conducting ground. This electric field is given by

$$de_z(j\omega,\rho) = \frac{I(j\omega)dz}{2\pi\varepsilon_o}\left(\frac{2-3\sin^2\theta}{j\omega R^3}+\frac{2-3\sin^2\theta}{cR^2}+j\omega\frac{\sin^2\theta}{c^2R}\right)e^{-j\omega R/c}. \quad (12.1)$$

See Fig. 12.2 for the relevant geometry. Now, when the ground is finitely conducting with a conductivity denoted by σ, a correction term must be introduced into the preceding equation. This correction term is a function of the height of the dipole, its frequency, the distance to the point of observation, and the ground conductivity. With this correction term the corresponding electric field over finitely conducting ground is given by

$$de_z(j\omega,\rho) = \frac{I(j\omega)dz}{2\pi\varepsilon_o}\left(\frac{2-3\sin^2\theta}{j\omega R^3}+\frac{2-3\sin^2\theta}{cR^2}+j\omega\frac{\sin^2\theta}{c^2R}\right)e^{-j\omega R/c}+S(z,\rho,\omega,\sigma). \quad (12.2)$$

An expression for this correction term was derived by Sommerfeld in 1906 [1] and is given in terms of an infinite integral that contains oscillating terms in the integrand. This oscillating nature of the integrand demands significant computational power in the numerical calculation of these integrals. Several scientists, notably Norton [2] and Bannister [3], attempted to derive an analytical function that can approximate Sommerfeld's integral. The results of these studies showed that for a very good approximation the function S can be written as

$$S = \frac{I(j\omega)dz}{2\pi\varepsilon_o}\frac{j\omega\sin^2\theta}{c^2R}\frac{1}{2}\{(R_v+1)+(1-R_v)a(z,\rho,j\omega,\sigma)-2\}e^{-j\omega R/c}. \quad (12.3)$$

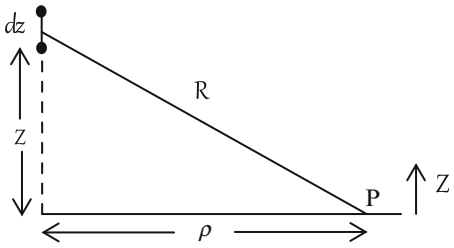

Fig. 12.2 Geometry relevant to parameters in field expressions of dipole. A dipole of length dz is located at height z above the ground plane. The distance to the point of observation P from the dipole is R, and the horizontal distance to the point of observation from the dipole is ρ (Figure created by author)

Substituting this into Eq. 12.2 gives the vertical electric field at ground level at point P due to a dipole located at height z as

$$de_z(j\omega,\rho) = \frac{I(j\omega)dz}{2\pi\varepsilon_o}\left(\frac{2-3\sin^2\theta}{j\omega R^3}+\frac{2-3\sin^2\theta}{cR^2}+j\omega\frac{\sin^2\theta}{c^2R}f(z,\rho,j\omega,\sigma)\right)e^{-j\omega R/c}. \tag{12.4}$$

In the preceding equations,

$$f(z,\rho,j\omega,\sigma) = \frac{1}{2}\{(R_v+1)+(1-R_v)a(z,\rho,j\omega,\sigma)\}, \tag{12.5}$$

$$R_v = \frac{\cos\theta-\Delta_1}{\cos\theta+\Delta_1} \tag{12.6}$$

$$\Delta_1 = \frac{k_o}{k_1}\left(1-\frac{k_o^2}{k_1^2}\sin^2\theta\right)^{1/2}, \tag{12.7a}$$

$$k_0 = \omega^2\mu_0\varepsilon_0 \tag{12.7b}$$

$$k_1 = -j\omega\mu_0(\sigma+j\omega\varepsilon_0\varepsilon_r) \tag{12.7c}$$

$$\cos\theta = z/R \tag{12.7d}$$

$$\eta = -\frac{j\omega R}{2c\,\sin^2\theta}\,[\cos\theta+\Delta_1]^2, \tag{12.8}$$

$$a(z,\rho,j\omega,\sigma) = 1-j(\pi\eta)^{1/2}e^{-\eta}\,erfc\left(j\eta^{1/2}\right). \tag{12.9}$$

In these equations, *erfc* stands for the complementary error function. The function $a(z,\rho,j\omega,\sigma)$ is the attenuation function corresponding to a dipole at height z over homogeneous and finitely conducting ground of surface impedance Δ_1. In the above equation ε_r is the relative dielectric constant of the soil, ε_0 is the relative permittivity of free space and μ_0 is the magnetic permeability of free space. These expressions can be calculated numerically with little difficulty. Note also that when the dipole is at ground level, i.e., $z=0$, $f(z,\rho,j\omega,\sigma)$ reduces to a.

Now, the lightning channel can be divided into a large number of elementary channel sections, each of which can be treated as an elementary dipole. Therefore, the total electric field generated by the return stroke can be obtained by summing the contribution from each dipole, taking into account the time delays. Hence, the total electric field due to a lightning return stroke over finitely conducting ground at a horizontal distance ρ can be written as

$$e_z(j\omega,\rho) = \int_0^H \frac{I(j\omega)}{2\pi\varepsilon_o}\left(\frac{2-3\sin^2\theta}{j\omega R^3}+\frac{2-3\sin^2\theta}{cR^2}+j\omega\frac{\sin^2\theta}{c^2R}f(z,\rho,j\omega,\sigma)\right)e^{-j\omega R/c}dz. \tag{12.10}$$

If the spatial and temporal variations in the return stroke current is known, then $I(j\omega)$ can be obtained through Fourier transformation.

Numerical evaluation of the integral in Eq. 12.10 gives the vertical electric field in the frequency domain (i.e., the electric field corresponding to a given frequency ω), and the time domain electric field can be obtained through inverse Fourier transformation. However, this calculation still involves a significant amount of numerical computation. To simplify the calculations further, Cooray and Lundquist [4] simplified this equation using the following arguments. As far as the propagation effects are concerned, the section of the electromagnetic field that is of interest is the part occurring within the first few microseconds. If the speed of propagation of the return stroke front is approximately 10^8 m/s, then the length of the channel that contributes to the radiation field during this time would be no larger than a few hundred meters. Thus, in the preceding equation, the attenuation function $f(z,\rho,j\omega,\sigma)$ can be replaced by $f(0,\rho,j\omega,\sigma)$, the attenuation function corresponding to a dipole located at ground level. The result is

$$\mathrm{e}_z(j\omega,\rho)=\int_0^H \frac{I(j\omega)}{2\pi\varepsilon_o}\left(\frac{2-3\sin^2\theta}{j\omega R^3}+\frac{2-3\sin^2\theta}{cR^2}+j\omega\frac{\sin^2\theta}{c^2R}a(\rho,j\omega,\sigma)\right)\mathrm{e}^{-j\omega R/c}dz. \tag{12.11}$$

Note that $f(0,\rho,j\omega,\sigma)$ is equal to $a(\rho,j\omega,\sigma)$. This equation can be inverse Fourier transformed directly into the time domain, giving the result

$$E_z(t,\rho)=E_{z,s}(t,\rho)+E_{z,i}(t,\rho)+\int_0^t E_{z,r}(t-\tau,\rho)A(\rho,\tau,\sigma)d\tau, \tag{12.12}$$

where $A(\rho,\tau,\sigma)$ is the inverse Fourier transformation of $a(\rho,j\omega,\sigma)$. In this equation, $E_{z,s}(t,\rho)$, $E_{z,i}(t,\rho)$, and $E_{z,r}(t,\rho)$ are the static, induction, and radiation field components, respectively, of the electric fields generated by the return stroke over perfectly conducting ground. These field components are given by

$$E_{z,s}(t,\rho)=\int_0^H \frac{dz}{2\pi\varepsilon_o}\left\{\frac{2-3\sin^2\theta}{R^3}\int_0^t i(z,\tau-R/c)d\tau\right\}, \tag{12.13}$$

$$E_{z,i}(t,\rho)=\int_0^H \frac{dz}{2\pi\varepsilon_o}\frac{2-3\sin^2\theta}{cR^2}\,i(z,t-R/c), \tag{12.14}$$

$$E_{z,r}(t,\rho)=\int_0^H \frac{dz}{2\pi\varepsilon_o}\frac{\sin^2\theta}{c^2R}\frac{\partial i(z,t-R/c)}{\partial t}. \tag{12.15}$$

According to the preceding equations, only the radiation field term is disturbed by propagation effects while the static and induction terms remain intact. In cases

where the distance to the point of observation is so large that it is only the radiation field that is of interest, Eq. 12.12 reduces to

$$E_z(t,\rho) = \int_0^t E_{z,r}(t-\tau,\rho)A(\rho,\tau,\sigma)d\tau. \tag{12.16}$$

As mentioned previously, in Eq. 12.16, $A(\rho,t,\sigma)$ is the inverse Fourier transformation of $a(\rho,j\omega,\sigma)$. To use Eq. 12.16, the function $A(\rho,t,\sigma)$ must be obtained for each conductivity and distance of interest by inverse Fourier transformation of $a(\rho,j\omega,\sigma)$. On the other hand, Wait [5] derived an analytical approximation for $A(\rho,t,\sigma)$ that can be used in Eq. 12.16 to further reduce the computational time. The analytical approximation to $A(\rho,t,\sigma)$ derived by Wait is given by

$$A(\rho,t,\sigma) \;= \frac{d}{dt}\left(1-\exp\left(-\frac{t^2}{4\zeta^2}\right)+2\beta(\varepsilon_r+1)\frac{Q(t/2\zeta)}{t}\right), \tag{12.17}$$

with

$$Q(x) = x^2\left(1-x^2\right)\exp\left(-x^2\right), \tag{12.18}$$

$$\beta = 1/\mu_o\sigma c^2, \tag{12.19}$$

$$\zeta^2 = \rho/2\mu_o\sigma c^3. \tag{12.20}$$

The third term inside the brackets of Eq. 12.17 takes account approximately of the displacement current in the ground. In many cases of practical interest, this term can be neglected, and the attenuation function in those cases is given by

$$A(\rho,t,\sigma) \;= \frac{d}{dt}\left(1-\exp\left(-\frac{t^2}{4\zeta^2}\right)\right). \tag{12.21}$$

Note that if the preceding expression is used in Eq. 12.16 to calculate the propagation effects, then the predicted propagation effects depend only on the parameter ρ/σ.

To illustrate the propagation effects, assume that the radiation field over perfectly conducting ground can be represented by a step function. Then the radiation field at different distances and conductivities are given by

$$E_z(t,\rho) = 1-\exp\left(-\frac{t^2}{4\zeta^2}\right). \tag{12.22}$$

The results corresponding to 50-km, 100-km, and 200-km propagation over finitely conducting ground of 0.001 S/m are depicted in Fig. 12.3a. Observe how the rise time of the step increases with increasing distance. Note that in this figure

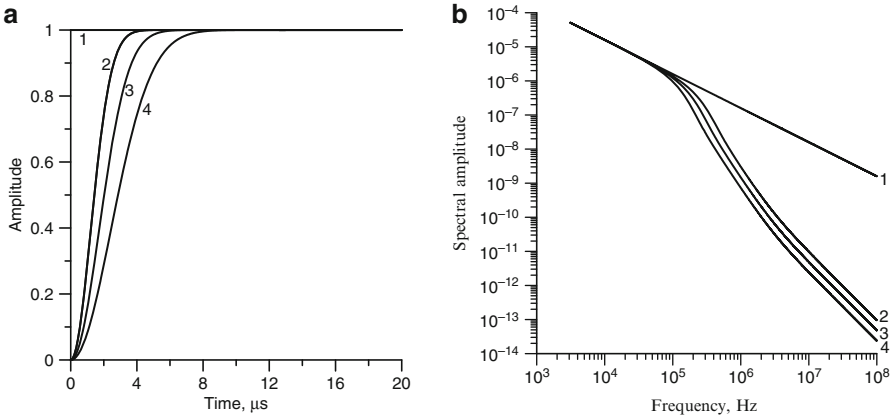

Fig. 12.3 (**a**) Effects of propagation on electric radiation field step as it propagates over various distances along finitely conducting ground. Observe that the field amplitude is normalized by removal of the inverse distance dependence of the radiation field. (1) Perfect conductor. (2) 50-km propagation over ground of 0.001 S/m conductivity. (3) 100-km propagation over ground of 0.001 S/m conductivity. (4) 200-km propagation over ground of 0.001 S/m conductivity. Note how the rise time of the step (which is zero over perfectly conducting ground) increases with increasing distance of propagation (Figure created by author). (**b**) Spectrum of electric fields shown in Fig. 12.3b. Note how the higher frequencies are attenuated with respect to lower frequencies as the signal propagates along finitely conducting ground (Figure created by the author)

the inverse distance reduction in the radiation field with distance is removed to illustrate the effects of propagation. In other words, if there were no propagation effects, then all the waveforms would resemble step functions with unit amplitude. The frequency spectrum corresponding to each waveform is shown in Fig. 12.3b. Note how the propagation effects remove the high frequencies from the signal and as a result the rise time of the signal increases.

Equation 12.12 can be used to calculate the propagation effects if the distance to the point of observation is larger than approximately 1 km. If the distance is less than that, then Eq. 12.10 must be used to obtain accurate results. However, even at these distances Eq. 12.12 can still generate reasonable results if the conductivity of the ground is higher than approximately 0.01 S/m. If the distance to the point of observation is less than approximately 200 m, then it is necessary to solve Sommerfeld's integrals to obtain accurate results. Even at these distances Eq. 12.10 can still provide a reasonable estimation of propagation effects. However, it is important to point out that at points of observation in the vicinity of the channel, the propagation effects modify only the electric field derivative. The propagation effects on the electric field signature itself are not very significant. Thus, if the propagation effects are needed only for the electric field, then the simplified equations presented earlier can be used to estimate them, even at distances close to the lightning channel.

12.3 Illustration of Propagation Effects

As explained earlier, propagation effects are caused by the selective attenuation of the higher frequencies in the electromagnetic field by finitely conducting ground. Thus, the fast features of lightning return stroke electromagnetic fields, such as the rise time, are more sensitive to propagation effects than the slow variations, such as the duration of the electromagnetic field. For the same reason, the electric field derivative is more sensitive to propagation effects than the electric field itself. For example, Fig. 12.4 shows how the electric field in the vicinity of the channel is modified by propagation effects. Observe that propagation effects do not modify the electric field (or the modifications are insignificant) in the vicinity of the channel.

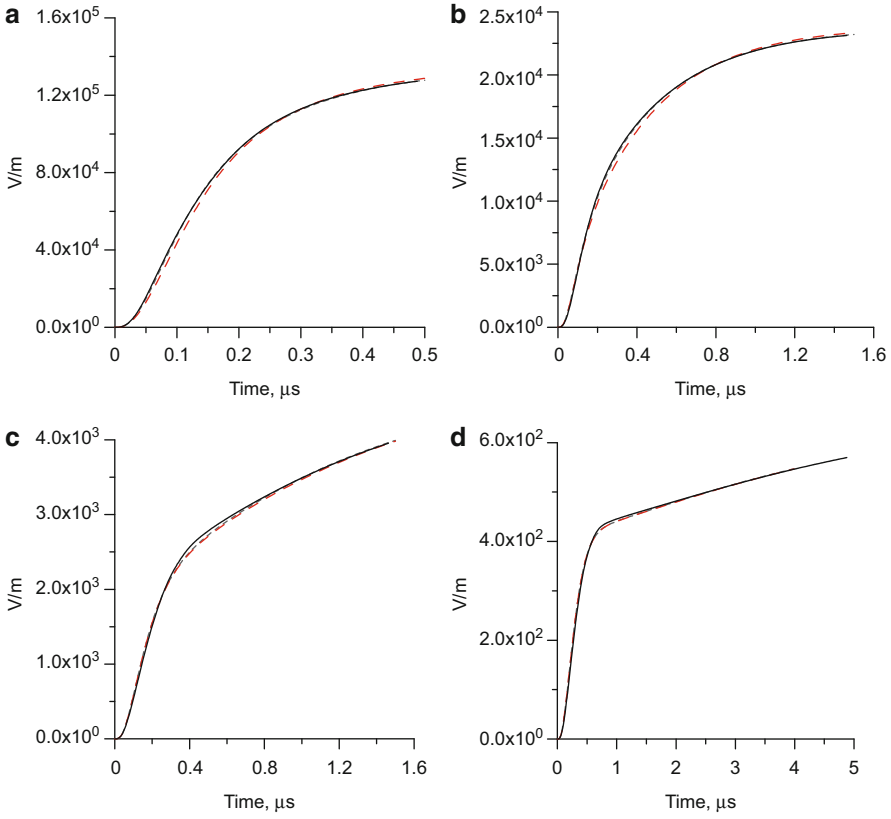

Fig. 12.4 Vertical electric field at ground level at (**a**) 10 m, (**b**) 50 m, (**c**) 200 m, and (**d**) 1000 m from lightning channel. *Solid line*: field obtained from Sommerfeld's equation; *short-dash line* (*blue*): Bannister approximation; *long-dash line* (*red*): Norton approximation. The conductivity of the ground is 0.001 S/m, and the relative dielectric constant is 5. Note that the equations of Bannister and Norton represent good approximations to Sommerfeld's exact integrals (Adapted from Cooray [6])

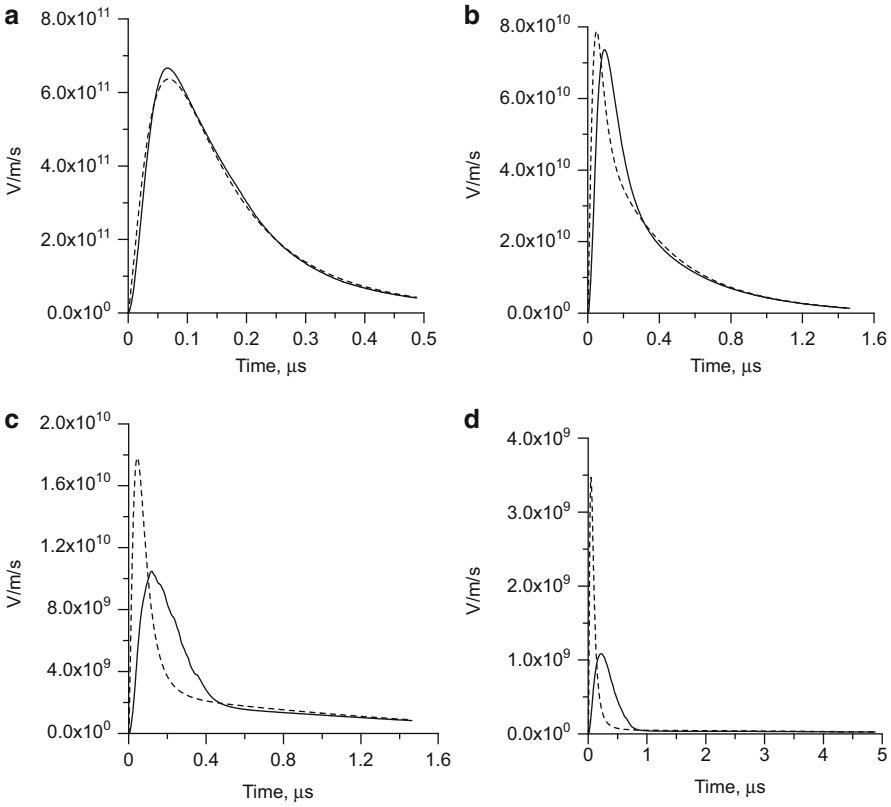

Fig. 12.5 Time derivative of vertical electric field at ground level at (**a**) 10 m, (**b**) 50 m, (**c**) 200 m, and (**d**) 1000 m from lightning channel. *Solid line*: time derivative of electric field over finitely conducting ground calculated using Sommerfeld's integrals; *dotted line*: time derivative of electric field over perfectly conducting ground. The conductivity of the ground is 0.001 S/m, and the relative dielectric constant is 5 (Adapted from Cooray [6])

On the other hand, Fig. 12.5 shows how the derivative of the electric field within approximately 1 km from the channel is modified by propagation effects. Note that propagation effects can significantly modify the peak amplitude of the electric field derivative. It is of interest to note that even very close to the return stroke channel the main contribution to the electric field derivative comes from the radiation field. In the radiation fields the electric field derivative and the magnetic field derivative have the same time signature, and they are related through the equation $dE/dt = c\, dB/dt$, where c is the speed of light. Thus, the amount of attenuation of the peak of the magnetic field derivative is the same as the amount of attenuation of the electric field derivative. Figure 12.6 shows the how the peak amplitude of the magnetic field derivative decreases with distance over finitely conducting ground.

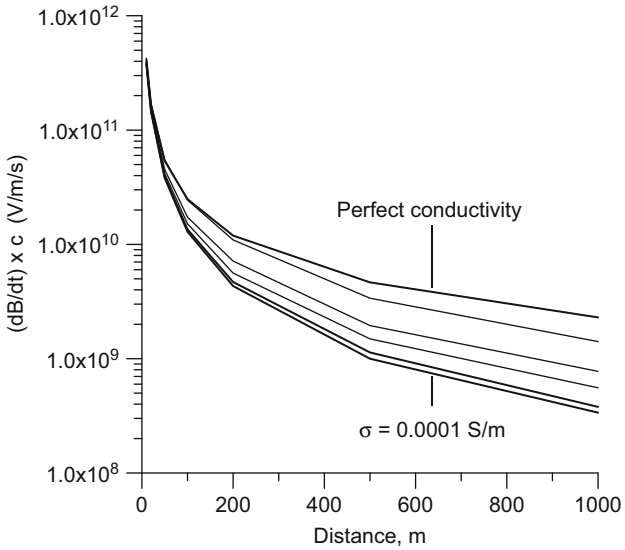

Fig. 12.6 Peak amplitude of magnetic field time derivative multiplied by speed of light in free space as function of distance for several conductivities. The results are shown for perfectly conducting ground: $\sigma = 0.01$ S/m, $\sigma = 0.001$ S/m, $\sigma = .0005$ S/m, $\sigma = 0.0002$ S/m, $\sigma = 0.0001$ S/m. Note that the peak amplitude at a given distance decreases as the conductivity decreases from infinity (perfect conductivity) to 0.0001 S/m. Since the derivative of the electric field is related to the derivative of the magnetic field through the equation $dE/dt = c\, dB/dt$ for distances larger than approximately a few tens of meters, where c is the speed of light, the results can be used to estimate the attenuation of dE/dt over finitely conducting ground (Adapted from [7])

For the reason described earlier, the data in Fig. 12.6 can also be used to obtain the attenuation of the electric field derivative at different distances and conductivities.

Figure 12.7 shows the long-distance propagation effects on the first return stroke radiation field, obtained using the model introduced by Nucci et al. [8] (Chap. 10), as it propagates over distances of 100 and 200 km over ground of 0.001 S/m conductivity. For reference, the radiation field that would be present over perfectly conducting ground is also shown in the figure. Observe how the rise time of the radiation field increases and its amplitude decreases with increasing distance. Observe also that at these distances the zero crossing time of the radiation field is not affected much by the propagation effects. Note again that in this figure the inverse distance reduction in the radiation field with distance is removed to illustrate the effects of propagation. In other words, if there were no propagation effects, all the waveforms would resemble a waveform over perfectly conducting ground.

The data shown so far are based on a theoretical calculation of propagation effects. In 1997, Cooray et al. [9] conducted an experiment in Denmark to study propagation effects experimentally. In the experiment, the electric fields from

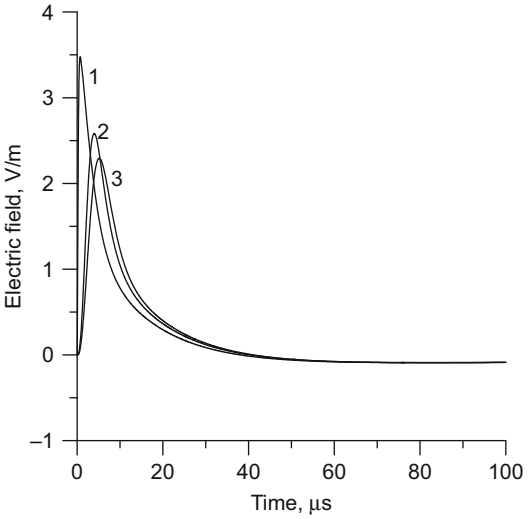

Fig. 12.7 Effect of long-distance propagation of radiation field of lightning return stroke as simulated by model of Nucci et al. [8]. (1) Perfect conductor. (2) 100-km propagation over ground of 0.001 S/m conductivity. (3) 200-km propagation over ground of 0.001 S/m conductivity. Note that the rise time of the radiation field increases and the peak amplitude of the radiation field decreases as the signal propagates over finitely conducting ground. Note that in the diagram the inverse distance dependence of the peak amplitude of the radiation field is removed to illustrate the effects of propagation. In other words, if the ground were perfectly conducting, then all the waveforms would have identical wave shapes and amplitudes. Note also that the zero crossing time of the radiation field is not modified significantly by propagation effects (Figure created by author)

lightning return strokes striking the sea were measured simultaneously at two stations, one located on the coast and the other situated 250 km inland. The propagation path of the electromagnetic fields from the strike point to the coastal station was over salt water, with the exception of the last 10–50 m. Since salt water is a good conductor, the propagation effects experienced by the radiation fields measured at the coastal station were negligible. Thus, the radiation field measured at the coastal station can be assumed to represent the electric radiation field that would be present over perfectly conducting ground. Figure 12.8 shows the electric radiation fields measured at the two stations and the radiation field calculated using Eq. 12.12, assuming the radiation field measured at the coastal station represented the one over perfectly conducting ground. Since the distance to the lightning flashes was more than 50 km from the coastal station, the measured portion of the field was pure radiation. Thus, only the third term in Eq. 12.12 is needed in the analysis. Note how the peak amplitude decreases and the rise time increases with propagation effects. The results also demonstrate that Eqs. 12.12 and 12.16, based on the simplified approximations, can be used with reasonable accuracy to calculate propagation effects.

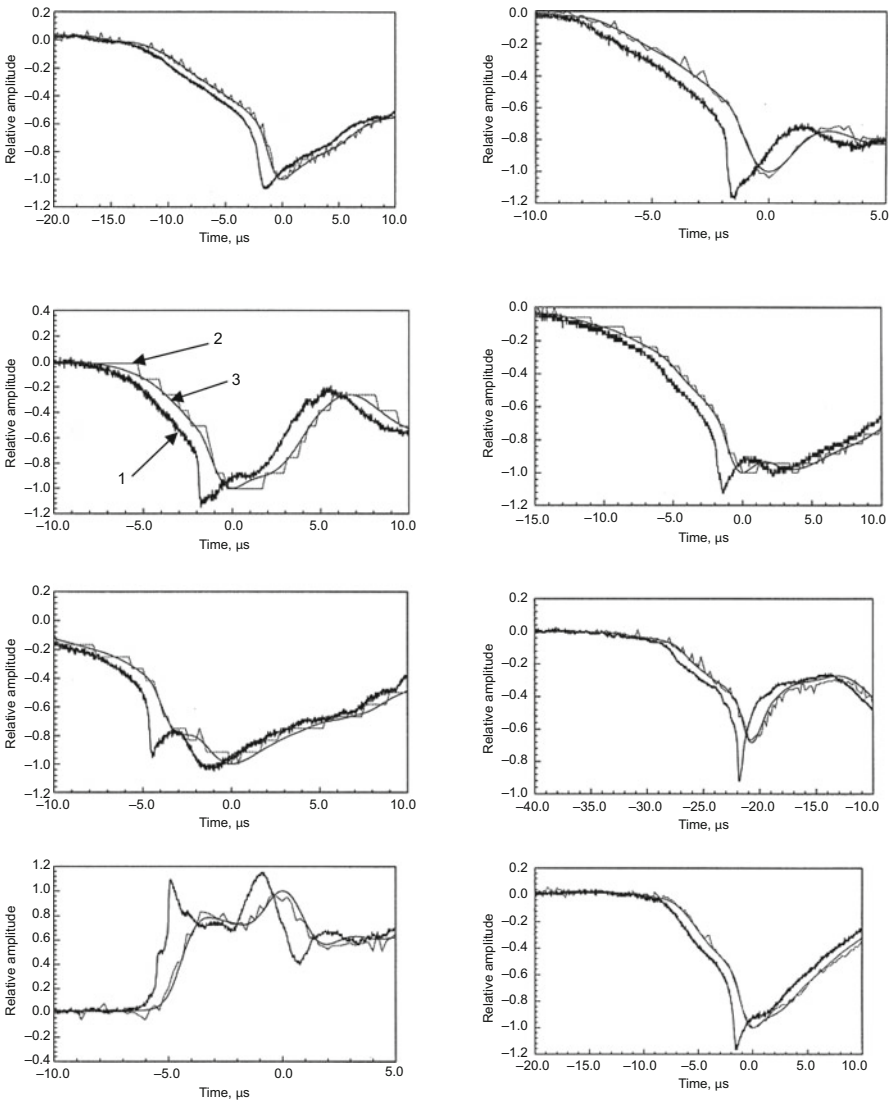

Fig. 12.8 Electric field measured at two stations, one a coastal station (*thick solid line*, marked 1), the other an inland station (*distorted line*, marked 2). The calculation based on theory as outlined in this chapter is shown by the *thin solid line* (marked 3). Note how the predictions based on theory agree with experimental data, indicating that Eq. 12.12 or 12.16 can be used to calculate propagation effects (Adapted from Cooray et al. [9])

References

1. Sommerfeld A (1909) Uber die Ausbreitung der Wellen in der drahtlosen Telegraphie. Ann Phys 28:665
2. Norton KA (1937) Propagation of radio waves over the surface of Earth and in the upper atmosphere, II. Proc IEEE 25:1203–1236
3. Bannister PR (1984) Extension of finitely conducting Earth-image-theory results to any range, NUSC technical report. Naval Underwater Systems Center, New London, Connecticut, USA
4. Cooray V, Lundquist S (1983) Effects of propagation on the risetime and the initial peaks of radiation fields from return strokes. Radio Sci 18:409–415
5. Wait JR (1956) Transient fields of a vertical dipole over homogeneous curved ground. Can J Phys 36:9–17
6. Cooray V (2008) On the accuracy of several approximate theories used in quantifying the propagation effects on lightning generated electromagnetic fields. IEEE Trans Antenna Propag 56(7):1960–1967. doi:10.1109/TAP.2008.924680
7. Cooray V (2009) Propagation effects due to finitely conducting ground on lightning-generated magnetic fields evaluated using Sommerfeld's integrals. IEEE Trans Electromagn Compat 51:526–531
8. Nucci CA, Mazzetti C, Rachidi F, Ianoz M (1988) On lightning return stroke models for LEMP calculations. Paper presented at 19th international conference on lightning protection, Graz, Austria
9. Cooray V, Fernando M, Sörensen T, Götschl T, Pedersen A (2000) Propagation of lightning generated transient electromagnetic fields over finitely conducting ground. J Atmos Sol Terr Phys 62:583–600